

Properties of single-layer graphene doped by nitrogen with different concentrations

Zongguo Wang and Shaojing Qin

*State Key Laboratory of Theoretical Physics,
Institute of Theoretical Physics, Chinese Academy of Science,
Beijing 100190, People's Republic of China **

Chuilin Wang

*China Center of Advanced Science and Technology,
P. O. Box 8730, Beijing 100190, China*

Abstract

Graphene has vast promising applications on the nanoelectronics and spintronics because of its unique magnetic and electronic properties. Making use of an ab initio spin-polarized density functional theory, implemented by the method of Heyd-Scuseria-Ernzerhof 06(HSE06) hybrid functional, the properties of nitrogen substitutional dopants in semi-metal monolayer graphene were investigated. We found from our calculation, that introducing nitrogen doping would possibly break energy degeneracy with respect to spin (spin symmetry breaking) at some doping concentrations with proper dopant configurations. The spin symmetry breaking would cause spin-polarized effects, which induce magnetic response in graphene. This paper systematically analyzed the dependence of magnetic moments and band gaps in graphene on doping concentrations of nitrogen atoms, as well as dopant configurations.

*Electronic address: wangzg@itp.ac.cn

I. INTRODUCTION

Since the discovery of graphene, a monolayer of carbons distributed in a honeycomb lattice[1], it has attracted the most attention of experimental[2–4] and theoretical[5–8] research due to its novel electronic properties. Graphene is the basic structure of all graphitic forms of carbon[9], and its unique two dimensional physical and chemical properties make graphene potential candidate for electronic device[10], field effect transistors(FET)[11], supercapacitors[12], and fuel cells[13–16]. Since material properties are related to its structures, substitutional doping is a powerful way to modify material properties, and it might be expected to have fundamentally different consequences. Chemical doping with B and N atoms is considered an effective method to improve the electronic properties of carbon materials, and forming *p*- and *n*-type carbon materials. It is more useful to get *n*-type graphene in comparison with the easily obtainable *p*-type graphene by adsorbates. Among various doping elements, nitrogen is the most promising candidate of doping elements in regulating the electronic properties of graphene, due to its similar atomic size, and its five valence electrons being easily formed strong covalence bonds with carbon atoms.

Experimental results[17, 18] have reported the various structure species of graphene with nitrogen dopants, and it has been shown that nitrogen is doped into the graphene structure in the form of graphitic dopants. Two important factors related to application of nanoelectronics and spintronics for graphene are the magnetic moments and the band gaps. In order to use graphene vastly in nanoelectronics, spintronics, and photovoltaic devices, it is important to study and exhibit electronic structures of modified systems. The research group in Georgia Tech. had announced that they successfully created the planar FET of graphene, and observed quantum interference effect, and revealed excellent transport properties in specified configurations of single graphene layers[19]. Graphene with planar structures will be the original materials for advanced industry. Many papers have been reported the effects of nitrogen doped graphene, but it is still unclear that how does nitrogen doping affect the magnetism and band gaps. Besides concentration, are there any other factors that affect the magnetism and band structure? Inspired by these questions, employing the spin-polarized density functional theory(DFT), we systematically analyzed the dependence of magnetic moments in graphene on doping concentrations of nitrogen atoms, as well as dopant configurations. We found from our calculation, that introducing nitrogen doping at some doping concentrations with proper dopant configurations will break sublattice symmetry, which thereafter would possibly break energy degeneracy with respect to spin (spin symmetry breaking).

The spin symmetry breaking would cause spin-polarized effects, which induce magnetic response in graphene.

II. COMPUTATION METHODS AND MODELS

The calculations are performed by using the Vienna Ab initio Simulation Package (VASP)[20, 21] with the spin-polarized DFT implemented. The generalized gradient approximation(GGA) in Perdew-Burke-Ernzerhof(PBE) form[22] is employed to calculate the exchange-correlation energy. The electron-ion interactions are described by the projector augmented wave (PAW)[23]. The Brillouin zone is sampled by a k-point mesh generated according to the Monkhorst-Pack scheme[24]. The dense k-point meshes $4 \times 4 \times 1$ and $7 \times 7 \times 1$ are used for the geometry optimizations and static structure energy calculation, respectively. A plane wave basis set is used and the kinetic-energy cutoff is taken as 400eV. The criterion of energy convergence is chosen to be less than 10^{-5} eV/atom. Heyd-Scuseria-Ernzerhof 06 (HSE06) hybrid functional has been shown as an accurate method to calculate band gaps for many semiconductors[25] including the graphene-related π system[26]. And it also provided lattice constants and local spin magnetic moments that were in good agreement with the experiment[27]. The cell shape was almost kept in its original form with its lengths and angles slightly changed during the calculations, and the atoms relaxed nearly in a plane with a very small negligible torsion of angle out of plane around C-N bonds.

We can construct a graphene sheet by periodically duplicating a supercell slab in both directions. Three different types of graphene sheet were calculated, i.e. a 2×2 supercell slab with 8 atoms, a 3×3 supercell slab with 18 atoms, and a 4×4 supercell slab with 32 atoms. In order to calculate a two dimensional graphene by the VASP which is basically designed for three dimensional crystal calculations, we intentionally enlarged the vertical distance between graphene sheets to 10(Å) of vacuum, so that the interaction between sheets reduced to a negligible value. The total energy is expressed as a function of the unit-cell volume around the equilibrium cell volume V_0 from experimental data. The calculated total energies were fitted to the Birch-Murnaghan equation of state to obtain the optimized lattice constant and a value of 2.469Å was obtained. The structure of the supercells is shown in Fig. 1.

Doping effect on the structures and the properties of graphene by a nitrogen mainly comes from the interactions between the doping atoms and its neighbors. The formation energy of N doping

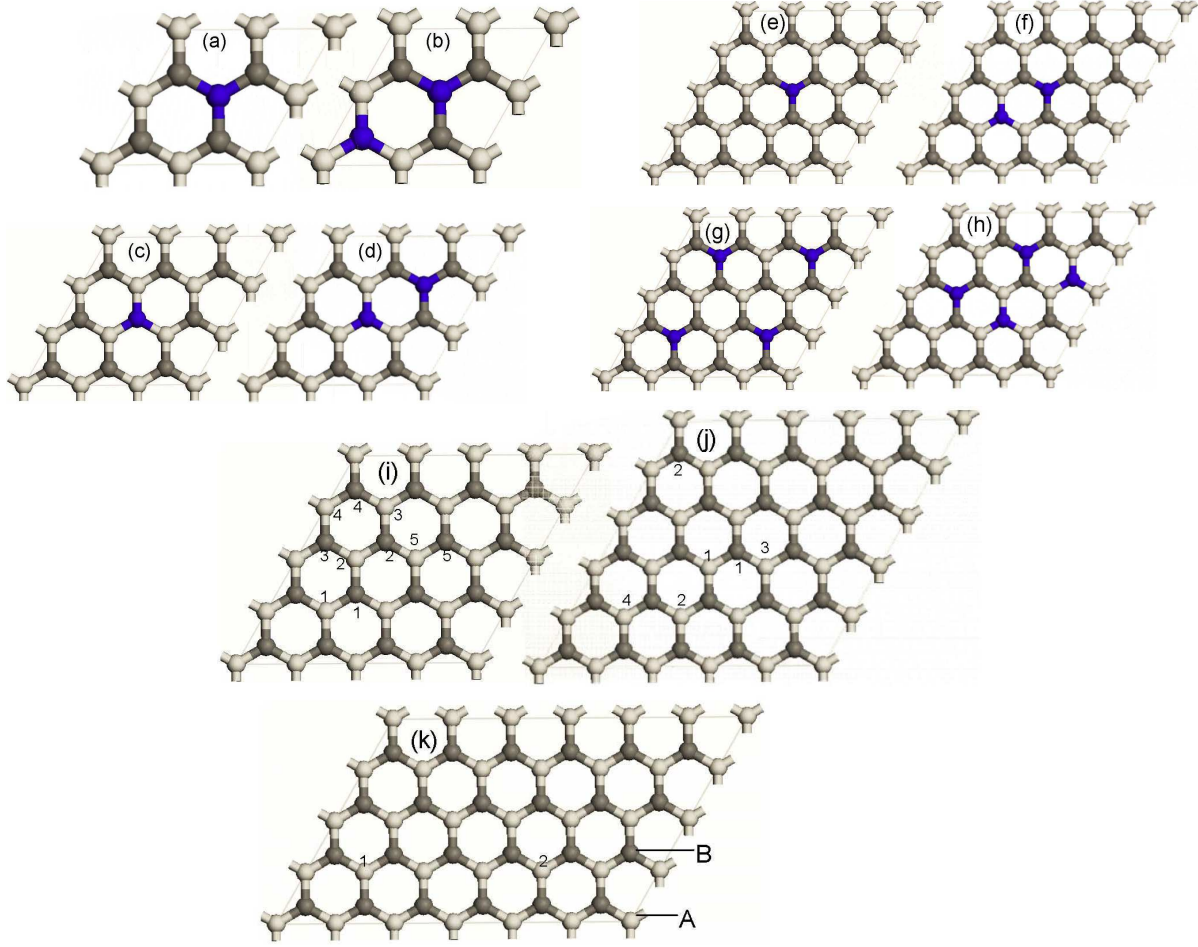


Fig. 1: Structures of various graphene sheets with different nitrogen doping configurations, the dark blue color represents nitrogen atoms. 1(a) and 1(b) sketch one and two nitrogen atoms doped into a 2x2 graphene supercell slab, respectively. 1(c) and 1(d) sketch the similar doping case in a 3x3 graphene supercell slab, respectively. 1(e) and 1(f) sketch the similar doping case too in a 4x4 graphene supercell slab, respectively. In Fig. 1(g), 4 supercells are displayed, each of which was shown in 1(a). 1(h) presents two couples of para nitrogen atoms doped into a 4x4 graphene supercell slab. 1(i-k) displays three different configurations: 1(i) two sets of potential substitutional doping sites in a 4x4 graphene supercell slab, 1(j) substitutional doping sites in a 5x5 graphene supercell slab, and 1(k) two nitrogens on the same lattice in a 6x4 graphene supercell slab.

E_f is defined by,

$$E_f = E_{dop} - E_{pure} + n(E_{\mu_C} - E_{\mu_N}) \quad (1)$$

where, $E_{dop(pure)}$ is the energy of doping(pure) system. E_{μ} is the chemical potential of C or N atom, and n is the substitutional number. The atomic energy of C and N atom is -1.316 and -3.114eV,

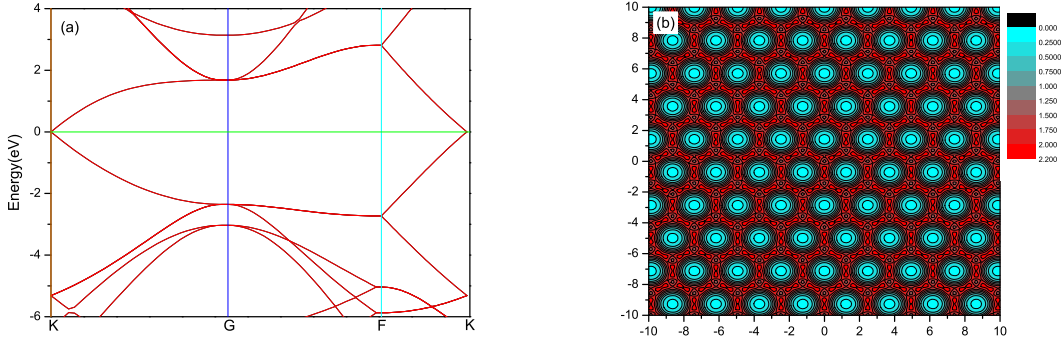


Fig. 2: 2(a) sketches the band structures of intrinsic 2x2graphene, 2(b) shows the total electron density($\rho_\alpha + \rho_\beta$) of pure 2x2graphene, and the plane is 20 by 20 Å across.

respectively. The difference between E_{μ_C} and E_{μ_N} equals to that between atomic energy of C and N atom. The value of E_f tells the difficulty to form a doped system. The smaller the value, the more stable the system.

To make sure the precision of the HSE complication, we compared our calculation results of the band gaps for 2x2 graphene with two nitrogen atoms adopted to the results which were reported[28], and we found that they were in excellent agreement. To assure the accuracy of our calculations, we also reproduced the results of a doped graphene system, one carbon atom was substituted by a nitrogen atom in 4x6supercell by other authors. The magnetism, the formation energy and the band structures were in good agreement with Reference [29], if using the same parameters. However, if we used more k points to get more precise results, the magnetism was not appeared, and correspondingly, larger Gaussian smearing destroyed the magnetic moment. Therefore, the magnetism had a dependence of temperature and k-points sampling[30].

III. RESULTS AND DISCUSSION

A. Electronic properties of intrinsic graphene

The calculated electronic properties of pure 2x2graphene are shown in Fig. 2(a) and 2(d). The electron distribution illustrates that, the sp^2 hybridization between two s and two p orbitals leads to a trigonal planar structure forming σ bonds between carbon atoms and a p orbital, which is perpendicular to the planar structure, and interacts covalently with neighboring carbon atoms, forming π bonds. It's well known that half-filled bands in transition elements have played significant role

in the physical characters of correlated systems, the strong interactions lead to a series of effects, including the magnetism, metal-semiconductor-insulator behaviors, etc.

The band structure shows that graphene is a semiconductor material with zero band gap. The Fermi level is set to zero energy, and the K point is the Dirac point of graphene. Graphene is non-magnetic due to the symmetry between spin up and down states. The nonmagnetic, zero gap, and massless are three of the most interesting features of graphene. So comparing the differences between intrinsic and doped graphene, as well as confirming the dependency of electronic properties on doping concentrations, are also meaningful features we should focus on.

B. N-graphene with one nitrogen doping per supercell

We started with doping cases of one nitrogen atom per graphene supercell, where one carbon atom was substituted by a nitrogen atom at different supercell sizes(Fig. 1(a),1(c), and 1(e)). Nitrogen impurities in π -conjugated systems can in principle affect the magnetic properties of the material[31]. While in our calculations, only some configurations showed spin polarization. The magnetic moments and formation energies of these three doped graphene systems are illustrated in the Table I. We found that only the 2x2 supercell with one nitrogen doping had apparent magnetism. It came from the interactions between itinerant π electrons. The results for smaller doping concentrations we studied were similar to those stated in Reference [32], that the ground state of substitutional nitrogen atoms with smaller doping concentrations was always nonmagnetic even when beginning with an initial magnetic guess configuration. The magnetism obtained from the HSE calculations was bigger than directly obtained from GGA or LDA due to HSE calculations employed a more correlated potential. From the calculated E_f values, it can be found that the systems in which a carbon atom was substituted by a nitrogen atom in smaller concentration were easier to form, because broking had smaller effect on the system along with the decrease of concentration.

To visualize the distribution of spin on the graphene sheet, the spin density in 2x2 periodic units on the graphene sheets is plotted in Fig. 3(a), and the nitrogen atom is at (0,0). This clearly indicates that the spin polarization mainly comes from the N atoms, and the C atoms which are located at the sublattice other than that the N atoms are sited at, as well. Other carbon atoms carry very small magnetic moments. Conventionally, magnetism is associated with d - or f -electrons, but, the calculated results in our case show that the magnetic moment is generated by (unpaired)

TABLE I: The doping concentrations, formation energies (E_f), magnetic moments of doping systems with one nitrogen atom, C-N distances, and electrons of nitrogen atoms for various supercells with one nitrogen doped.

systems	2x2	3x3	4x4
Doping concentration(at.%)	12.5	5.56	3.125
$E_f(eV \cdot atom^{-1})$	3.852	3.724	3.636
magnetic moment per supercell (μ_B)	0.608	0.06	0
C-N distance(\AA)	1.426	1.418	1.414
Electronic charges of Nitrogen(e)	6.323	6.328	6.267

$2p$ electrons of nitrogen atoms. The bonding status has been changed accordingly, and the inter-nuclear length of the C-C bonds around the nitrogen atom has also been modified. The distances between C and N atoms for different supercells are summarized in Table I, where the original distance between atoms is 1.425\AA . The length of C-N bonds is about the same as that of the original C-C bonds, so are the bond angles. A Bader analysis on charge number of each atom in the system was performed to qualify the charge transfers. The results of the nitrogen atom charges in three supercells are presented in Table I. The electron number being greater than $5e$ for N atom suggested that partial electron charges were transferred from the neighbor C atoms to the more electronegative N atoms. Nitrogen doping results in increasing positive charge on a carbon atom adjacent to nitrogen atoms and in positive shifting of Fermi energy at the apex of the Brillouin zone of graphene. As indicated by Reference [33], the fermi level is shifted $0.9 eV$ in $3.125\text{at.}\%$ N-doped system. So the charge distributions became nonuniform, and the electrons were gathered around the N atoms which is the possible source of spin density symmetry breaking. The breaking is especially visible in the case of 2×2 supercell.

All of these doped systems with one nitrogen per supercell exhibited n-type doping metallic electronic properties, the band structures of these doped systems were depicted in Fig. 3(d)-3(f). In Fig. 3(d), we found one majority spin band was located inside the interval of the minority spin band and crossed the fermi level, which indicated the strong spin polarization. The majority spin band mainly came from the coupling interactions between the doping atoms and the carbon atoms in the ortho and para positions of nitrogen occupied sites. It gave the magnetic moment of $0.608\mu_B$ per supercell. From 3(e) to 3(f), the spin polarization became smaller, and in some

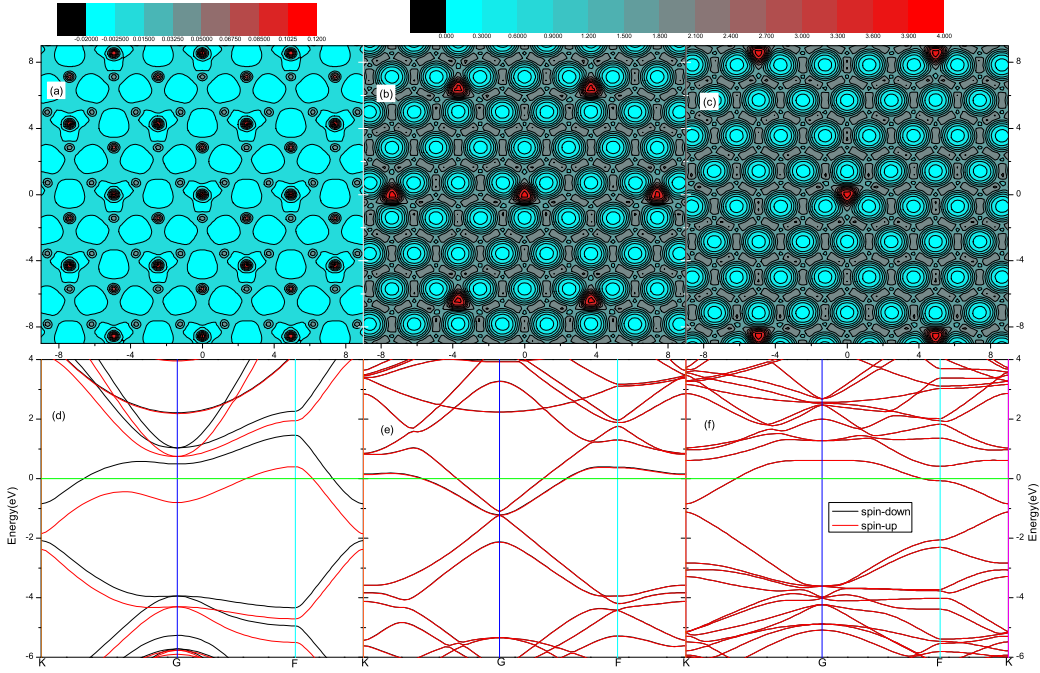


Fig. 3: Spin/total electron densities and band structures of N-doped graphene systems with different concentrations. 3(a) and 3(d) for 2x2 graphene supercell, 3(b) and 3(e) for 3x3 graphene supercell, 3(c) and 3(f) for the 4x4 graphene supercell. Particularly, 3(a) describes the spin electron densities($\rho_\alpha - \rho_\beta$) on the (001) plane(i.e., the graphene sheet surface), 3(b) and 3(c) present the total electron densities($\rho_\alpha + \rho_\beta$), and the planes of 3(a)-(c) are 18 by 18 Å across. 3(d)-3(f) are the band structures of different doping systems with the same energy scales from $-6eV$ to $4eV$.

case disappeared (which can be neglected), i.e., the magnetic moment was significant only in the case that one nitrogen doped into 2x2 graphene supercell. Table I listed various values of the magnetic moments for different graphene supercells. And Table II listed the atomic magnetic values for single nitrogen atom in 2x2 supercell, the values characterized the itinerant properties of π electrons.

C. N-graphene with two nitrogen doping per supercell

We also studied the two nitrogen doping case in one supercell, by using the same methods. Two carbon atoms in a six-number ring were replaced by two nitrogen atom. Comparing the formation energy of doping atoms at three different positions in a ring, i.e. ortho-, meta-, and para-positions,

TABLE II: The atomic magnetic values for 2x2 supercell with one nitrogen atom doped.

atom on A sublattice	C_{A_1}	C_{A_2}	C_{A_3}	N
magnetic moment (μ_B)	0.012	0.010	0.011	-0.146
atom on B sublattice	C_{B_1}	C_{B_2}	C_{B_3}	C_{B_4}
magnetic moment (μ_B)	-0.193	-0.101	-0.101	-0.100

TABLE III: The doping concentrations, formation energies (E_f), magnetic moments of doping systems with two nitrogen atom, C-N distances, and electrons of nitrogen atoms for various supercells with two nitrogen atoms doped.

system	2x2	3x3	4x4
Doping concentration(at.%)	25	11.11	6.25
$E_f(eV \cdot atom^{-1})$	3.627	3.625	3.674
magnetic moment(μ_B)	0	0	0
C-N distance(Å)	1.427	1.418/1.425	1.414/1.422
Electronic charges of Nitrogen(e)	6.284/6.355	6.287/6.358	6.297/6.367

the case with two nitrogen atoms in a para position had the smallest formation energy and had the most stable structures(illustrated in the Table III). This was in good agreement with the reported results that the interaction energy curve had a local minima when two nitrogen atoms in a para position[28]. We calculated the three different cases, where the carbon atoms in a ring were substituted by two nitrogen atoms in 2x2, 3x3, and 4x4 graphene supercells respectively. The substitutional positions were described in Fig. 1(b), 1(d) and 1(f) for 2x2, 3x3 and 4x4supercells. We reproduced the band structure calculation for the 2x2 graphene supercell with two nitrogen atoms doping, which was reported by Reference [28], and obtained the similar results. The formation energies and Bader electrons for the nitrogen atom for these three doped graphene systems are listed in Table III. The average electrons that the nitrogen atoms possessed were greater than that of one nitrogen doping, more charges had been transferred.

Calculated results for different configurations were presented in Fig. 4. There were no spin polarizations in any sizes of supercells with two nitrogen atoms doping, so we plotted the total electron densities of these three supercells in Fig. 4(a)-4(c) to investigate the bonding effects after nitrogens were doped into the supercells in comparison with the intrinsic graphene in Fig. 2(a). We

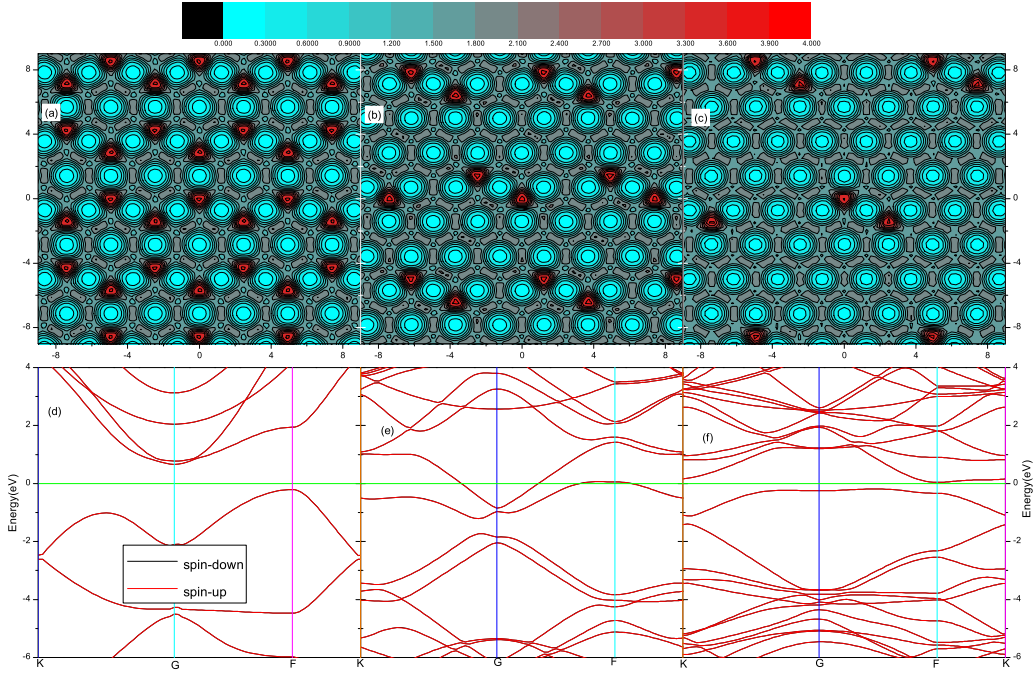


Fig. 4: (Total($\rho_\alpha + \rho_\beta$) electron densities and band structures of doped graphene systems with two nitrogen atoms doped into different units, where 4(a) and 4(d) for 2x2 graphene sheet, 4(b) and 4(e) for 3x3 graphene sheet, 4(c) and 4(f) for the 4x4 graphene sheet. Particularly, 4(a), 4(b), and 4(c) present the total electron densities on the (001) plane(i.e., the graphene sheet surface) and all of them have the same scales. The planes for them are 18 by 18 Å across. 4(d)-4(f) describe the band structures of different doping systems with the same energy scales from -6eV to 4eV.

can see from the figures, that the electron density was increased from Fig.4(a) through Fig.4(c), and more electrons were gathered in the vicinity of a nitrogen atom. The three carbon atoms which were closed to a nitrogen atom are located in the same isosurface. This is the evidence that the original $C = C$ bonds had been broken to form new C-N bonds in the hexagonal structure. There are no magnetic moment existed in any local atoms. We also can see that Fig.4(a) gives a perfect continuously symmetric six-ring.

Both of 2x2 and 4x4 graphene supercell sheet with two nitrogen doping atoms have exhibited n-type semiconductor behavior with a small band gap. But a 3x3 graphene supercell shows metal electronic properties whose band structures were depicted in Fig. 4(d)-4(f). All of 4(d)-4(f) showed symmetry between majority and minority spin. The band gaps were 1.0 and 0.23eV for

2x2 and 4x4 graphene supercell with two nitrogen doping atoms, respectively, in agreement with the existing value of 0.96eV in 2x2 sheet[28]. Reference [28] had explained the band gap was produced because the hopping between N p_z orbitals in the configurations that led to the larger dispersion of the highest occupied band. Doping mechanism will make a system disorder. And we know that ordered structures are more stable in lower temperatures. Symmetric doping may lead to a stable system. From our calculations, we can suspect that a graphene supercell with two para nitrogen atoms in a ring as well as with multiplicity of two para nitrogen atoms in a ring would not be spin polarized. The units which are the $n \times n$ (n is not divided by 3) with para nitrogen doping will produce a band gaps.

D. N-graphene with four nitrogen atoms doping per supercell

From the above discussion, we learnt that electronic structures were differently depend on the different concentrations and the species. The next question is whether systems that have the same doping concentration(12.5%) but different configurations have the same results. Two configurations with four nitrogen atoms doped into 4x4graphene sheets were investigated and compared with that of one nitrogen atom doped into 2x2 graphene sheet. The one case is four carbon atom sites in different ring were substituted by nitrogen atoms(shown in Fig. 1(h)). The formation energy of doping for 4x4 graphene sheet with four nitrogen atoms is 3.731eV/atom from Eq. (1), suggesting that the formation energy of N-doping has no direct relation with concentrations. It has a small magnetic moment due to the coupling between the closer nitrogen atoms in two pairs of para positions. And it has a small gap. The other one is four times 2x2 graphene with one nitrogen doped(shown in Fig. 1(g)). The formation energy(3.845eV/atom) of doping and band structures were the same with that of 2x2 graphene with one nitrogen doped. And the magnetic moment is $2.5\mu_B$, nearly four times that of 2x2 graphene with one nitrogen. These results from the two substitutes indicate that the magnetic and electronic properties are not only relied on the concentration but also relied on the configurations of the nitrogen arranged.

E. Exploring the origin of the magnetism

To reveal the origin of the magnetism, we calculated various structures differed by doping positions of two nitrogen atoms in a 4x4 graphene supercell, which were shown in Fig. 1(i). A and

TABLE IV: The formation energies (E_f), magnetic moments of doping systems doped by two nitrogen atoms for 4x4 graphene sheet with increasing N-N distances.

distance	sublattice site	$E_f(eV \cdot atom^{-1})$	magnetic moment(μ_B)
$\frac{\sqrt{3}}{3}a$	A_1B_1	4.174	0
a	A_1A_2	3.837	0.75
$\frac{2\sqrt{3}}{3}a$	A_1B_3	3.674	0
$\frac{\sqrt{21}}{3}a$	A_1B_2	3.744	0
$\sqrt{3}a$	A_1A_4	3.734	0.125
$2a$	A_1A_3	3.759	0.625
$\frac{\sqrt{39}}{3}a$	A_1B_4	3.627	0
$\frac{4\sqrt{3}}{3}a$	A_1B_5	3.657	0

B were labeled in aqua and grey colors, respectively, representing substituted sites in different sublattices for the honeycomb lattice. For the 4x4 graphene supercell, the largest distance between two doping nitrogen atoms is $\frac{4\sqrt{3}}{3}a < 3a$, where a is the lattice constant for the unit cell. The magnetic moments, doping formation energy, along with the distance between two doping atoms are shown in Table IV. From the table, we found three interesting phenomena in a 4x4 graphene supercell. The first, when two nitrogen atoms replaced two carbon atoms along the zigzag direction in the same sublattice, and the distance between two doping atoms is $\leq 2a$, there will be an approximate $0.7\mu_B$ magnetic moment. The second, when the doping was occurred in the armchair direction, there would be negligible even no magnetic moment. The third, when two carbon atoms in different sublattices were doped by nitrogen atoms, there would be no spin polarization.

By analyzing the two magnetic conditions A_1A_2 and A_1A_3 , we found both of them produce some nearly zero-magnetism sublattice lied between them. Other carbon atoms in B lattice show FM coupling with N atoms, whereas the carbon atoms in the same sublattice with N atoms show AFM coupling. This phenomenon satisfies the RKKY-like coupling in graphene for on-site impurities[34]. And the magnetic moments on the two nitrogen atoms for the former are larger than that for the later. From the forming energies plotted in various distance of dopants, there are two minimum values for A_1B_3 and A_1B_4 cases. The configurations agree with that reported by others in 12x12 supercell[28].

In order to obtain large relative distance between two nitrogen atoms, we use 5x5 and 4x6

TABLE V: The formation energies (E_f), magnetic moments of doping systems doped by two nitrogen atoms for 5x5 and 6x4 graphene sheet with increasing N-N distances.

system	distance	sublattice site	$E_f(eV \cdot atom^{-1})$	magnetic moment(μ_B)
5x5	$\frac{\sqrt{3}}{3}a$	A_1B_1	4.172	0
5x5	a	A_1A_3	3.805	0
5x5	$\sqrt{7}a$	A_3A_4	3.67	0
5x5	$\frac{5\sqrt{3}}{3}a$	A_2B_2	3.515	0
6x4	3a	A_1A_2	3.685	0

supercells, which were shown in Fig. 1(j) and (k), to calculate the dependence of magnetism on distances of two impurities sites. Four different configurations($A_1B_1, A_1A_3, A_3A_4,$ and A_2B_2) in a 5x5 graphene sheet and one(A_1A_2) in a 4x6 graphene are calculated. The results are shown in Table V. From Table IV, we can infer the magnetism vanishes with the increasing distance between two doping nitrogen atoms in any direction and sublattice. The two same case(orth and meta positions) for 4x4 and 5x5, a little small doping forming energy are obtained for 5x5 system, since it has smaller doping concentration. Two nitrogen atoms substitute two same lattice along zigzag direction with 3a distance in a 6x4 graphene has zero magnetic moment. Therefore, the magnetism vanishes with the decreasing of doping concentration, and the increasing of the distance between two nitrogen atoms.

It's important to note that, we have reproduced the calculation that one carbon atom was substituted by one nitrogen atom for 4x6 supercell, if we use smaller k-points which used in Reference [29], the magnetic moment was $0.556\mu_B$, similar to the reference result of $0.46\mu_B$. The difference stems from the HSE and DFT calculation stated in Reference [27]. But, if we increase the number of k-mesh for more precise results, no any magnetism has been found.

The above analyses strongly implied that the sublattice symmetry is crucial to induction of magnetic moments. The sublattice symmetry breaking will possibly break energy degeneracy with respect to spin (spin symmetry breaking), which is the origin of spin-polarization, and the occurrence of magnetic response.

IV. CONCLUSION

Making use of the first-principles density functional theory (DFT) based methods, we calculated N-graphene properties in various doping concentrations and configurations. The calculated results showed that the graphene with one nitrogen doped in any size of graphene supercells, the graphene with two nitrogen atoms doped in a 3x3 graphene supercell exhibited n-type metal behavior, and the graphene with two nitrogen atoms doped into a 2x2 and a 4x4 supercell had band gaps of 1.0 and 0.23eV, respectively. Especially, for a 2x2 graphene system with two nitrogen atoms doped, had a similar band structure as silicon. Four nitrogen atoms (two para) doped into a 4x4 graphene also opened band gaps. From these features, we proposed a way to tailor band gaps according to the size of graphene unit and atom configurations.

The systems with single nitrogen atom doped in a 2x2 graphene sheet displayed spin polarizations, and spin couplings were disappeared for some special configurations. We also found graphene with two nitrogen doping atoms at para positions in a ring did not have spin polarizations for any sizes of graphene supercells. From our analysis of magnetism, interactions between nitrogen atoms and carbon atoms led to the magnetism, and the magnetism was closely related to the sublattice symmetry and distance between nitrogen atoms. We should point out sublattice symmetry is significantly important, which can be seen from the comparisons between a 4x4 graphene sheet with two couples of para nitrogen atoms and one nitrogen doped into 2x2 graphene sheet, as well as the conditions listed in the Table IV.

Our results provided a comprehensive analysis about N-doped graphene, which should be a hint for producing graphene-based devices and other multiple applications as well.

-
- [1] K. S. Novoselov, a. K. Geim, S. V. Morozov, D. Jiang, Y. Zhang, S. V. Dubonos, I. V. Grigorieva, and a. a. Firsov, *Science* (New York, N.Y.) **306**, 666 (2004), ISSN 1095-9203, URL <http://www.ncbi.nlm.nih.gov/pubmed/15499015>.
 - [2] S. Latil, V. Meunier, and L. Henrard, *Physical Review B* **76**, 1 (2007), ISSN 1098-0121, URL <http://link.aps.org/doi/10.1103/PhysRevB.76.201402>.
 - [3] L. M. Malard, J. Nilsson, D. C. Elias, J. C. Brant, F. Plentz, E. S. Alves, a. H. Castro Neto, and M. a. Pimenta, *Physical Review B* **76**, 1 (2007), ISSN 1098-0121, URL <http://link.aps.org/doi/10.1103/PhysRevB.76.201401>.

- [4] C. Riedl and U. Starke, *Physical Review B* **76**, 1 (2007), ISSN 1098-0121, URL <http://link.aps.org/doi/10.1103/PhysRevB.76.245406>.
- [5] a. Sakhaee-Pour, M. T. Ahmadian, and R. Naghdabadi, *Nanotechnology* **19**, 085702 (2008), ISSN 0957-4484, URL <http://www.ncbi.nlm.nih.gov/pubmed/21730733>.
- [6] A. Mattausch and O. Pankratov, *Physical Review Letters* **99**, 1 (2007), ISSN 0031-9007, URL <http://link.aps.org/doi/10.1103/PhysRevLett.99.076802>.
- [7] E. Hwang, S. Adam, and S. Sarma, *Physical Review Letters* **98**, 2 (2007), ISSN 0031-9007, URL <http://link.aps.org/doi/10.1103/PhysRevLett.98.186806>.
- [8] D. Xiao, W. Yao, and Q. Niu, *Physical Review Letters* **99**, 1 (2007), ISSN 0031-9007, URL <http://link.aps.org/doi/10.1103/PhysRevLett.99.236809>.
- [9] a. K. Geim and K. S. Novoselov, *Nature materials* **6**, 183 (2007), ISSN 1476-1122, URL <http://www.ncbi.nlm.nih.gov/pubmed/21048788>.
- [10] N. Levy, S. a. Burke, K. L. Meaker, M. Panlasigui, a. Zettl, F. Guinea, a. H. Castro Neto, and M. F. Crommie, *Science (New York, N.Y.)* **329**, 544 (2010), ISSN 1095-9203, URL <http://www.ncbi.nlm.nih.gov/pubmed/20671183>.
- [11] F. Xia, D. B. Farmer, Y.-M. Lin, and P. Avouris, *Nano letters* **10**, 715 (2010), ISSN 1530-6992, URL <http://www.ncbi.nlm.nih.gov/pubmed/20092332>.
- [12] L. L. Zhang, R. Zhou, and X. S. Zhao, *Journal of Materials Chemistry* **20**, 5983 (2010), ISSN 0959-9428, URL <http://xlink.rsc.org/?DOI=c000417k>.
- [13] D. R. Kauffman and A. Star, *The Analyst* **135**, 2790 (2010), ISSN 1364-5528, URL <http://www.ncbi.nlm.nih.gov/pubmed/20733998>.
- [14] B. Seger and P. V. Kamat, *The Journal of Physical Chemistry C letters* **113**, 7990 (2009).
- [15] L. Qu, Y. Liu, J.-B. Baek, and L. Dai, *ACS nano* **4**, 1321 (2010), ISSN 1936-086X, URL <http://www.ncbi.nlm.nih.gov/pubmed/20155972>.
- [16] Y. Shao, S. Zhang, C. Wang, Z. Nie, J. Liu, Y. Wang, and Y. Lin, *Journal of Power Sources* **195**, 4600 (2010), ISSN 03787753, URL <http://linkinghub.elsevier.com/retrieve/pii/S0378775310002892>.
- [17] D. Geng, S. Yang, Y. Zhang, J. Yang, J. Liu, R. Li, T.-K. Sham, X. Sun, S. Ye, and S. Knights, *Applied Surface Science* **257**, 9193 (2011), ISSN 01694332, URL <http://linkinghub.elsevier.com/retrieve/pii/S0169433211008610>.
- [18] L. Zhao, R. He, K. T. Rim, T. Schiros, K. S. Kim, H. Zhou, C. Gutierrez, S. P. Chock-

- alingam, C. J. Arguello, L. Palova, et al., *Science* **333**, 999 (2011), ISSN 0036-8075, URL <http://www.sciencemag.org/cgi/doi/10.1126/science.1208759>.
- [19] R. Quhe, J. Zheng, G. Luo, Q. Liu, R. Qin, J. Zhou, D. Yu, S. Nagase, W.-N. Mei, Z. Gao, et al., *NPG Asia Materials* **4**, e6 (2012), ISSN 1884-4057, URL <http://www.nature.com/doi/10.1038/am.2012.10>.
- [20] T. U. Wien and W. Hauptstrage, *Physical Review B* **49**, 14251 (1994).
- [21] G. Kresse and J. Furthmüller, *Computational Materials Science* **6**, 15 (1996).
- [22] J. Perdew, K. Burke, and M. Ernzerhof, *Physical review letters* **77**, 3865 (1996), ISSN 1079-7114, URL <http://www.ncbi.nlm.nih.gov/pubmed/10062328>.
- [23] P.E. Blochl, *Physical Review B* **50**, 17953 (1994).
- [24] H. J. Monkhorst and J. D. Pack, *Physical Review B* **13**, 5188 (1976).
- [25] K. Hummer, J. Harl, and G. Kresse, *Physical Review B* **80** (2009), ISSN 1098-0121, URL <http://link.aps.org/doi/10.1103/PhysRevB.80.115205>.
- [26] O. Hod, V. Barone, and G. Scuseria, *Physical Review B* **77**, 1 (2008), ISSN 1098-0121, URL <http://link.aps.org/doi/10.1103/PhysRevB.77.035411>.
- [27] M. Marsman, J. Paier, a. Stroppa, and G. Kresse, *Journal of physics. Condensed matter : an Institute of Physics journal* **20**, 064201 (2008), ISSN 0953-8984, URL <http://www.ncbi.nlm.nih.gov/pubmed/21693863>.
- [28] H. Xiang, B. Huang, Z. Li, S.-H. Wei, J. Yang, and X. Gong, *Physical Review X* **2**, 1 (2012), ISSN 2160-3308, URL <http://link.aps.org/doi/10.1103/PhysRevX.2.011003>.
- [29] R. Singh and P. Kroll, *Journal of physics. Condensed matter : an Institute of Physics journal* **21**, 196002 (2009), ISSN 0953-8984, URL <http://www.ncbi.nlm.nih.gov/pubmed/21825500>.
- [30] D. W. Boukhvalov and Y.-W. Son, *Chemphyschem : a European journal of chemical physics and physical chemistry* **722**, 1463 (2012), ISSN 1439-7641, URL <http://www.ncbi.nlm.nih.gov/pubmed/22416041>.
- [31] I. Hagiri, N. Takahashi, and K. Takeda, *J.Phys.Chem.A* **108**, 2290 (2004).
- [32] Y. Ma, a. Foster, a. Krasheninnikov, and R. Nieminen, *Physical Review B* **72**, 1 (2005), ISSN 1098-0121, URL <http://link.aps.org/doi/10.1103/PhysRevB.72.205416>.
- [33] L. S. Panchakarla, K. S. Subrahmanyam, S. K. Saha, A. Govindaraj, H. R. Krishnamurthy, U. V. Waghmare, and C. N. R. Rao, *Advanced Materials* **21**, 4726 (2009), ISSN 09359648, URL <http://doi.wiley.com/10.1002/adma.200901285>.

[34] A. M. Black-Schaffer, *Physical Review B* **81**, 1 (2010), ISSN 1098-0121, URL <http://link.aps.org/doi/10.1103/PhysRevB.81.205416>.